ARCHIVES OF ACOUSTICS
36, 1, 65–76 (2011)
DOI: 10.2478/v10168-011-0006-z

Active Noise-Vibration Control using the Filtered-Reference LMS Algorithm with Compensation of Vibrating Plate Temperature Variation

Krzysztof MAZUR, Marek PAWEŁCZYK

Silesian University of Technology,
Institute of Automatic Control
Akademicka 16, 44-100 Gliwice, Poland
e-mail: Krzysztof.Jan.Mazur@polsl.pl
Marek.Pawelczyk@polsl.pl

(*received April 30, 2010; accepted October 29, 2010*)

Vibrating plates have been recently used for a number of active noise control applications. They are resistant to difficult environmental conditions including dust, humidity, and even precipitation. However, their properties significantly depend on temperature. The plate temperature changes, caused by ambient temperature changes or plate heating due to internal friction, result in varying response of the plate, and may make it significantly different than response of a fixed model. Such mismatch may deteriorate performance of an active noise control system or even lead to divergence of a model-based adaptation algorithm.

In this paper effects of vibrating plate temperature variation on a feedforward adaptive active noise reduction system with the multichannel Filtered-reference LMS algorithm are examined. For that purpose, a thin aluminum plate is excited with multiple Macro-Fiber Composite actuators. The plate temperature is forced by a set of Peltier cells, what allows for both cooling and heating the plate. The noise is generated at one side of the plate, and a major part of it is transmitted through the plate. The goal of the control system is to reduce sound pressure level at a specified area on the other side of the plate.

To guarantee successful operation of the control system in face of plate temperature variation, a gain-scheduling scheme is proposed to support the Filtered-reference LMS algorithm.

Keywords: active noise-vibration control, active structural acoustic control, adaptive control, gain scheduling, temperature influence.

1. Introduction

Vibrating plates have been gaining significant interest in recent years. They can be used either as sources of secondary sound for classical active noise control

applications, or actuators for active noise-vibration control or active structural acoustic control. Different control strategies can be employed (Hansen, Snyder, 1997; Fahy, Gardonio, 2007; Elliott, 2001; Pietrzko, 2009). Also passive and semi-active methods using Shunted Piezoelectric Patches are in significant interest (Tawfik, Baz, 2004; Pietrzko, 2009). However, the current state of the art in this field lacks reports on plate temperature influence on sound generation by the vibrating plate and influence on active noise or vibration reduction results.

In this paper active structural acoustic control (ASAC) with an acoustic sensor is considered for a rectangular clamped plate. In the literature it is also referred to as the active noise-vibration control (ANVC) (Fahy, Gardonio, 2007). This shape of plate is suitable for common possible applications. Many authors also investigate other shapes including circular plates (Leniowska, 2006; Leniowska, Kos, 2009) triangular plates (Barański, Szela, 2008) or joined rectangular plates (Wiciak, 2008). Also different sizes of plates were investigated, for instance microplates by Lizhong and Zhentong (2009).

The primary noise is generated in a small-dimensional acoustically isolated enclosure. A major part of the noise is transmitted to a laboratory room through a clamped aluminum plate of dimensions 400 mm×500 mm×1 mm (see Fig. 1). The goal of the control system is to reduce sound pressure level at a specified area in the laboratory room by exciting the plate to vibrations.

Three Macro-Fiber Composite (MFC) patches are attached to the plate. They are used as actuators for active control. Bending work mode, d_{33} effect MFCs are used (MFC, 2010).

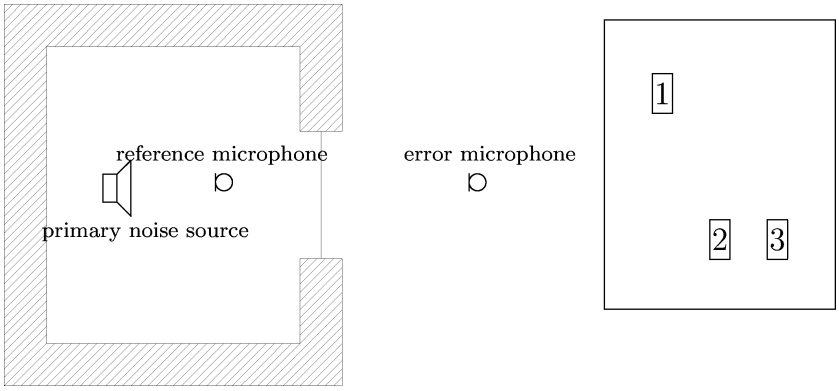

Fig. 1. Test environment (left), and MFC patches positions on plate (right).

To easily change plate temperature six Peltier cells are installed on its edges. For measuring temperature the LM35 ("LM35 Precision Centigrade...", 2000) sensors are used. An adaptive multichannel feed-forward control system structure (see Fig. 2) with one reference signal acquired by a microphone located close to the noise source in the enclosure is chosen. An error microphone is located in the

laboratory room at the area of interest to provide information about primary and secondary sound interference results.

2. Control algorithm

In this paper a multichannel feedforward structure is used for control as presented in Fig. 2. In this figure $x(i)$ is the reference signal, $r_1(i)$–$r_3(i)$ are filtered-reference signals, $e(i)$ is the error signal, $d(i)$ is the primary noise at the point of interest, W_1–W_3 are control filters, P stands for the primary path representing the acoustic space between the reference and error microphones, S_1–S_3 are the secondary paths with the control signals being the inputs and the error signal as the output, the symbols with hats stand for models of respective paths, and E is the reference path.

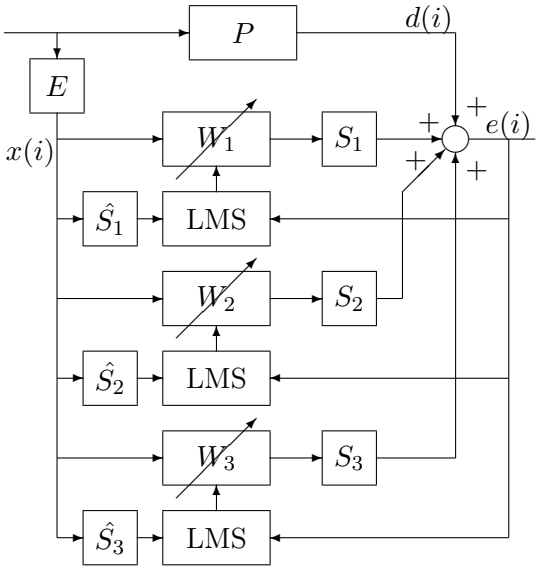

Fig. 2. Control system diagram.

The Normalized Leaky Filtered-reference LMS algorithm is applied for online adaptation of three FIR control filters used to drive the three selected MFC patches (Fig. 2) (Pawełczyk, 2005). Control filter parameters are then updated according to:

$$\mathbf{w}_j(i+1) = \alpha \mathbf{w}_j(i) - \mu \frac{\mathbf{r}_j(i)}{\mathbf{r}_j^{\mathrm{T}}(i)\mathbf{r}_j(i) + \zeta} e(i), \tag{1}$$

where $0 \ll \alpha < 1$ is the leakage coefficient, μ is the convergence coefficient, and ζ is a parameter protecting against division by zero in case of lack of excitation. In

this equation $\mathbf{r}_j(i) = [r_j(i), r_j(i-1), \ldots, r_j(i-(N-1))]^{\mathrm{T}}$ is a vector of regressors of the filtered-reference signal, with elements obtained as:

$$r_j(i) = \hat{\mathbf{s}}_j(i)^{\mathrm{T}}\mathbf{x}(i), \tag{2}$$

where $\hat{\mathbf{s}}_j(i) = [\hat{s}_{j,0}(i), \hat{s}_{j,1}(i), \ldots, \hat{s}_{j,M-1}(i)]$ is a model of the j-th secondary path filter impulse response, $\mathbf{x}(i) = [x(i), x(i-1), \ldots, x(i-(M-1))]^{\mathrm{T}}$ is a vector of regressors of the reference signal. The order of FIR path models is $M = 320$ for all experiments.

The j-th control signal value is equal to:

$$u_j(i+1) = \mathbf{w}_j(i)^{\mathrm{T}}\mathbf{x}(i), \tag{3}$$

where $\mathbf{w}_j(i) = [w_{j,0}(i), w_{j,1}(i), \ldots, w_{j,N-1}(i)]^{\mathrm{T}}$ is a vector of parameters of the j-th control filter and $\mathbf{x}(i) = [x(i), x(i-1), \ldots, x(i-(N-1))]^{\mathrm{T}}$ is a vector of last N reference signal values. The order of FIR control filters is $N = 512$ for all experiments. If the number of sensors and actuators is much higher, e.g. for larger plates, it might be justified to apply the cluster control as discussed by Tanaka (2009).

For the Filtered-reference LMS algorithm without leakage to converge with probability one it suffices and is necessary that the actual paths differ in phase from their models by less than $\pi/2$ for all frequencies, under some assumptions (Elliott, 2001). One of the assumptions require that the reference signal is sufficiently exciting. To mitigate such requirement for deterministic noise the leakage factor less than one can be introduced. It corresponds to introducing a trade-off to minimization of the instantaneous value of the squared error signal and suppressing excessive rise of control filter parameters. Therefore, the algorithm with leakage exhibits a potential to stabilize its operation even in case of larger phase errors between the paths and their models. This effect is found particularly useful for analysis of control system performance in case of plate temperature variation, which is the main subject of this paper. It is worth mentioning here that there are also other ways to investigate convergence of this algorithm, which include effect of the noise to be reduced (Larsson *et al.*, 2009).

Response of any secondary path significantly depends on plate temperature as presented in Fig. 3. It changes even more than 30 dB for some frequencies, mainly because of a plate bulge. However, fortunately the bulge improves the plate response for the 100–200 Hz band, which was originally very poor and the sound power radiated was low. As it also follows from Fig. 3, phase response changes are much higher than theoretically required for convergence of the Filtered-reference LMS algorithm without leakage.

The plate temperature has been set using six Peltier cells. Because of non-ideal thermal conductivity of aluminum such approach can lead to different plate temperature gradient than caused by internal friction or ambient temperature. However, it allows for fast heating and cooling of the plate, even below the ambient temperature.

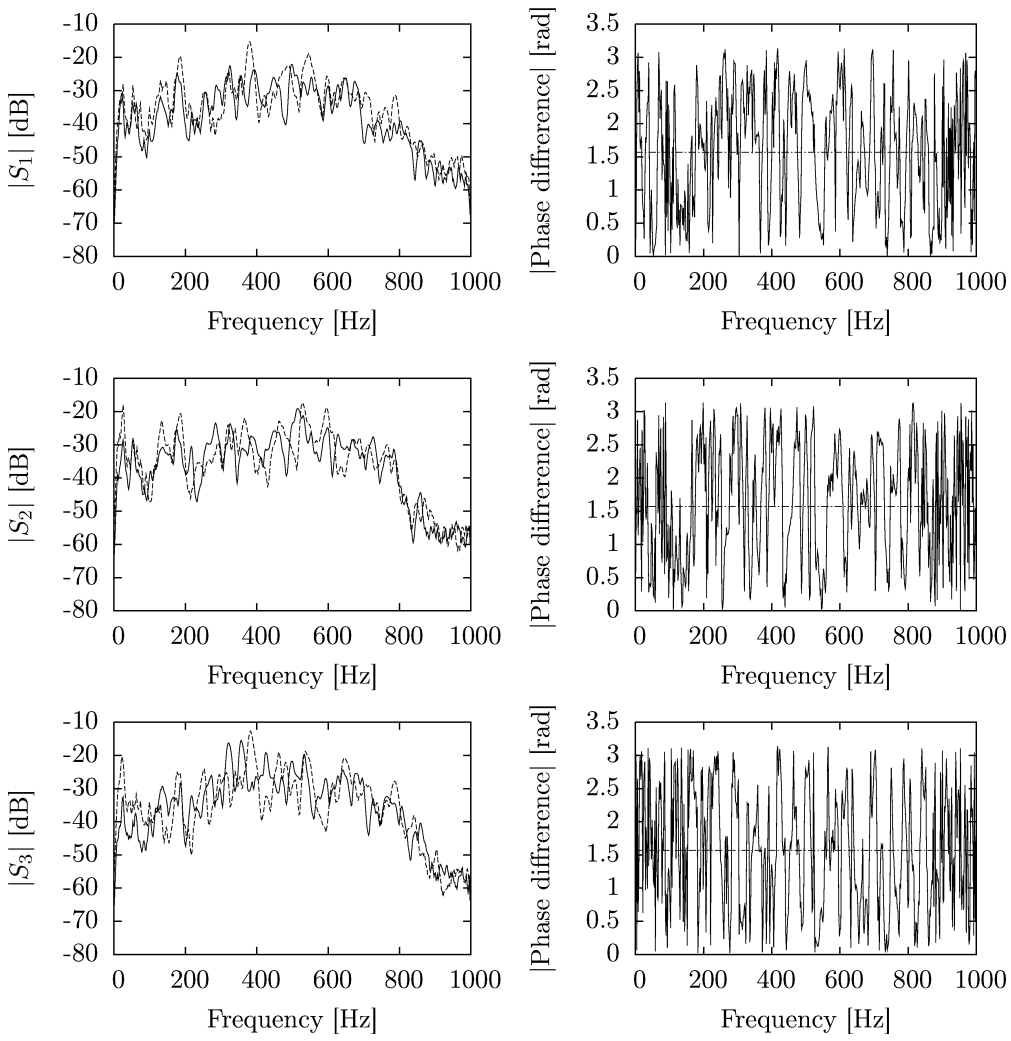

Fig. 3. Amplitude frequency characteristics (left) of the secondary paths for 24°C (solid) and 28°C (dashed), and absolute phase difference (right; the horizontal line represents the phase error threshold at $\pi/2$).

The Peltier cells (see Fig. 4) use the Peltier effect to transfer heat between two sides (Heaton, 1963). The amount of transferred heat is proportional to electrical current. There are also two additional effects: Joule heating proportional to squared electrical current and thermal conductance proportional to temperature difference. Because of Joule heating Peltier cells are more effective for heating.

One side of Peltier cell is connected to a plate. The temperature of second side is stabilized by a water circuit. The water temperature is later stabilized by exchanging its heat with the air.

Fig. 4. Peltier cell.

An average of two LM35 sensors has been considered as the plate temperature (Fig. 5). The position of sensors has been chosen based on infrared thermal images of plate.

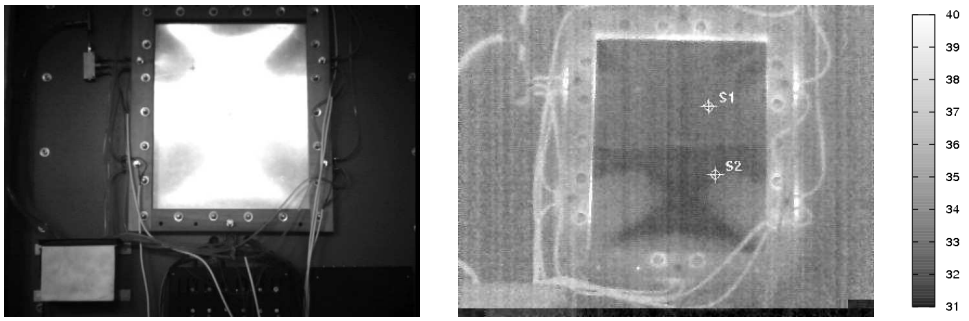

Fig. 5. Plate at 32°C (left), and its infrared image converted to temperature estimation with position of temperature sensors (right).

3. Temperature-based gain scheduling

To assure convergence of the adaptation algorithm, models of the reference paths could be identified on-line. Such approach may cause, however, stability problems and in most cases additional noise for identification should be generated (Kuo, Morgan, 1996) or the simultaneous equation method could be used (Fujii *et al.*, 2010). In this paper another approach is used. A set of models identified off-line for different plate temperatures is stored in a look-up table, and the appropriate triple S_1–S_3 is chosen on-line based on the temperature measurement as an indicator (see Fig. 6). Similarly, the algorithm tuning parameters α, μ and ζ or Eq. (1) could be updated, if necessary.

A common assumption for gain scheduling is that correct parameters are static functions of the indicator signal. However, the plate exhibits a thermal hysteresis. The dynamical differences between secondary path responses after heating to different temperatures and then cooling to a reference temperature are significant, although much smaller than taken at different temperatures (Fig. 7). The differences between models at the same temperature are too high to guarantee convergence of the Filtered-reference LMS algorithm without leakage, but even a small leak set by $\alpha = 0.9999$ has sufficed for successful operation.

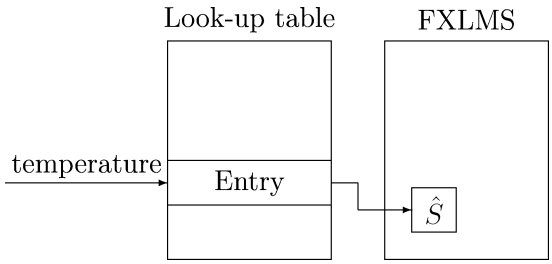

Fig. 6. Gain scheduling scheme for secondary path model.

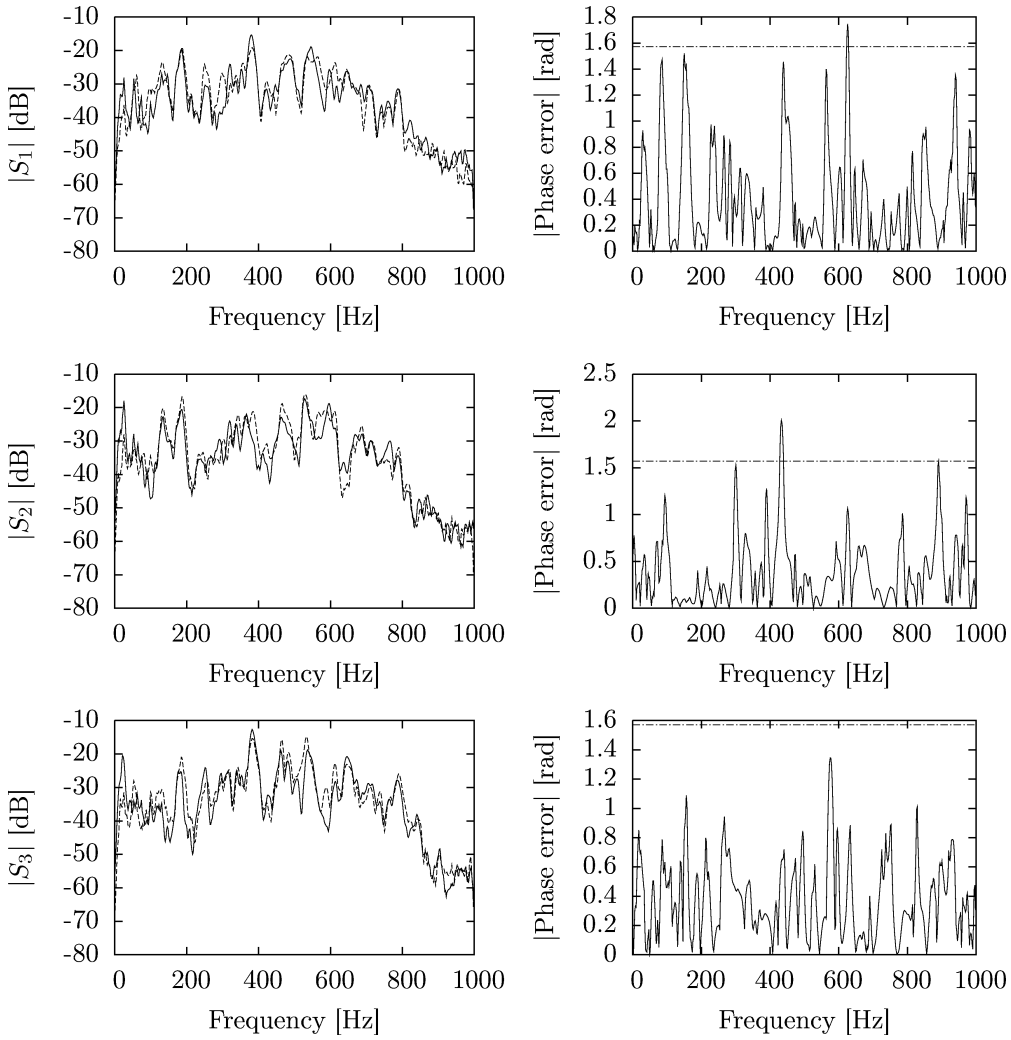

Fig. 7. Amplitude frequency characteristics (left) of the secondary paths for 28°C after heating from 24°C (solid line) and for 28°C after cooling from 34°C (dashed line), and absolute phase difference (right; the horizontal line represents the phase error threshold at $\pi/2$).

4. Tonal noise reduction

The primary noise was generated by a loudspeaker placed in the enclosure. Individual tones of frequencies from the range of 250 Hz to 500 Hz with 10 Hz step were investigated. The algorithm with three different secondary path models stored in a look-up table was tested. The first model was identified for the ambient temperature of 24°C. The second model was identified after heating the plate to 28°C. For another test, the plate was heated to 34°C and then it was coled down to 28°C. Afterwards, the third model was identified.

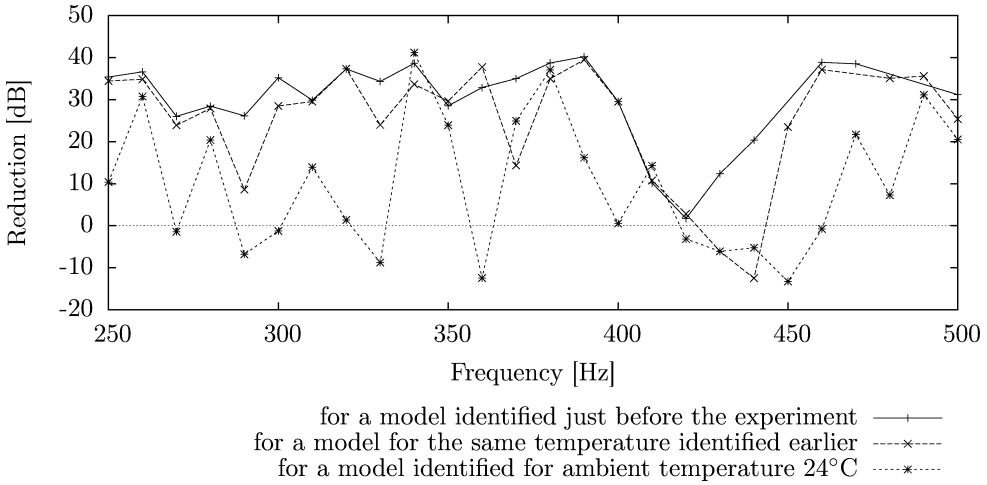

Fig. 8. Results of tonal noise reduction for 28°C, $\alpha = 0.9999$, $\mu = 0.1$, $\zeta = 0.001$.

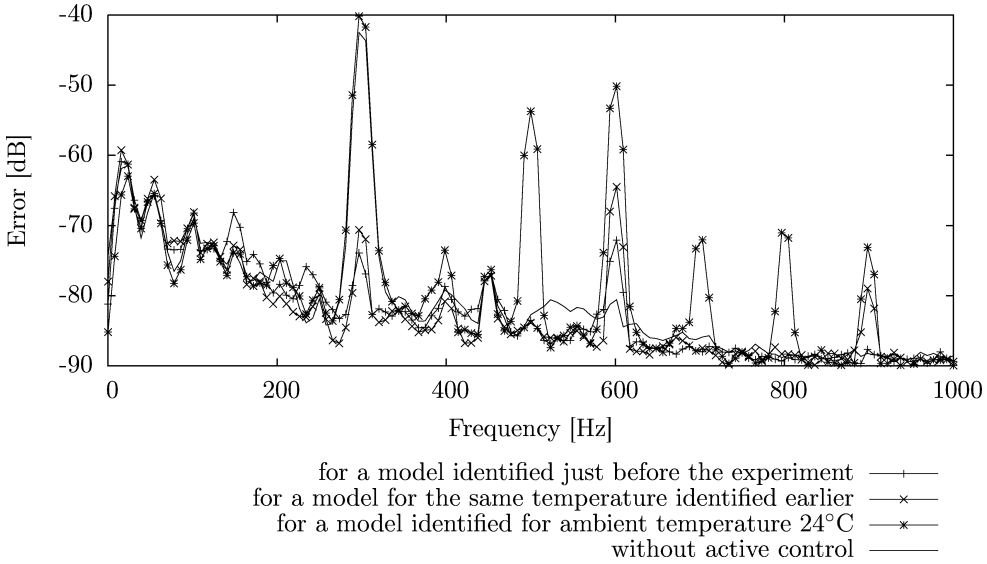

Fig. 9. Power Spectrum Density for 300 Hz tonal noise for 28°C, $\alpha = 0.9999$, $\mu = 0.1$, $\zeta = 0.001$.

It has been found that a temperature change of 4°C suffices to cause stability problems for the Filtered-reference LMS algorithm without secondary path model update, even with a leakage of $\alpha = 0.9999$ (Fig. 8). The noise reduction level was limited mostly due to the leakage, resulting in a compromise between reduction of the error signal mean square value, and suppressing the filter gain. Without leakage, noise reduction to the acoustic floor level has been achieved.

Figure 9 shows Power Spectrum Density (PSD) for the 300 Hz tone. Control system with model for the ambient temperature 24°C was unstable. The dominating tone was not reduced and additional frequencies were generated. For models identified for 28°C temperature (both just before the experiment as well as after the heating and cooling), the primary noise was successfully reduced. Generation of harmonics of the 300 Hz frequency was caused by plate nonlinearity.

5. Fan noise reduction

Further experiments have concerned control of a real-world noise. Figure 10 shows results obtained for a fan noise contributed by a dominating tone of 330 Hz and a wideband component.

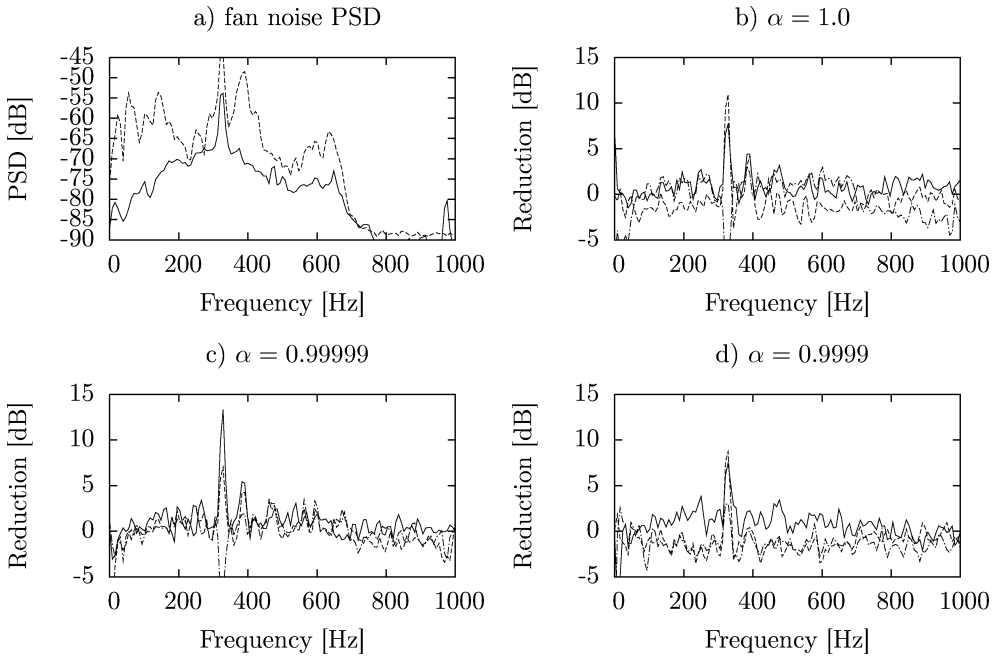

Fig. 10. a) Power Spectral Density of the signal for the primary noise loudspeaker (solid) and the primary noise at error microphone (dashed); b), c), d) The results of fan noise reduction for 28°C for different valus of parameter α for a model identified just before experiment (solid line), for the same temperature before heating and cooling (hashed line), for ambient temperature 24°C (dash-dotted).

For ambient temperature of 24°C the leak factor of $\alpha = 0.9999$ has been required to provide reduction of the dominating tone. For both $\alpha = 1.0$ and $\alpha = 0.9999$, exchanging secondary path models based on the temperature measurement has increased reduction of the dominating tone, but the wideband component has been reduced worse. Noise reduction levels are shown in Table 1.

Table 1. Noise reduction level for fan noise at 28°C.

Model	$\alpha = 0.9999$	$\alpha = 0.99999$	$\alpha = 1$
Global noise reduction [dB]			
Model identified just before experiment	2.4	1.9	3.1
Pre-identified model for 28°C	1.9	3.1	1.2
Model for 24°C	−0.8	−2.7	−2.4
A-weighted global noise reduction [dB]			
Model identified just before experiment	2.6	2.3	3.7
Pre-identified model for 28°C	2.1	3.5	1.4
Model for 24°C	−1.0	−2.0	−2.2
310–340 Hz band noise reduction [dB]			
Model identified just before experiment	7.6	7.5	7.9
Pre-identified model for 28°C	7.5	6.8	7.5
Model for 24°C	−1.7	−6.6	−8.5

For all cases control system based on the secondary path model identified before the experiment for the ambient temperature failed. Results for the system with the pre-identified model for 28°C, and the model identified just before experiments are comparable, except wideband reduction for $\alpha = 1$, where results with the former model are worse.

6. Conclusions

In this paper influence of plate temperature variation on convergence and performance of the feedforward active noise control system with the Filtered-reference LMS algorithm has been considered. The plate temperature has been set with Peltier cells it has been monitored with LM35 sensors. It has been shown that even temperature change of 4°C may result in divergence of the algorithm. Relatively large leakage should be introduced to the algorithm to stabilize its operation, what significantly deteriorates the performance. Since the ambient temperature changes much more, such system cannot be accepted. It has been thus proposed to employ a gain scheduling scheme. Secondary path models for different plate temperatures have been identified. Then, based on plate temperature evaluation during control, relevant secondary path models are selected from a look-up table and used for the adaptation algorithm. Then, with even a very small leakage of $\alpha = 0.99999$ the control system behaves satisfactorily.

A similar simple gain scheduling scheme can be applied to shift the reduction area by providing information about its location and a set of secondary path models.

So huge differences between secondary path responses for different temperatures, as disclosed in this paper, can lead to control signal saturation. The system after temperature change might be unable to provide sufficient signal power required for effective control. Further research is required to cope with this problem.

Acknowledgments

The research reported in this paper has been partially supported by the Ministry of Higher Education and Science, Poland, under the grant no. N N514 232037 in 2010. The authors would also like to thank Mr. A. Kochan for helping with the laboratory set up.

References

1. Brański A., Szela S. (2008), *Improvement of effectiveness in active triangular plate vibration reduction*, Archives of Acoustics, **33**, 4, 521–530.
2. Elliott S. (2001), *Signal Processing for Active Control*, Academic Press, London.
3. Fahy F., Gardonio P. (2007), *Sound and Structural Vibration*, Second edition, Elsevier, Oxford.
4. Fujii K., Kashihara K., Muneyasu M., Morimoto M. (2010), *Study on application of cascade connection of recursive and non-recursive filters to noise control filter*, Proceedings of 17th International Congress of Sound and Vibration, Cairo.
5. Hansen C.H., Snyder S.D. (1997), *Active Control of Noise and Vibration*, E & FN Spon, London.
6. Heaton A.G. (1963), *Thermoelectrical cooling: Material characteristics and applications*, Proceedings of the Institution of Electrical Engineers., **110**, 7, 1277–1287.
7. Kuo S.M., Morgan D.R. (1996), *Active Noise Control Systems*, John Wiley & Sons, Inc., New York.
8. Larsson M., Johansson S., Claesson I., Håkansson L. (2009), *A Module Based Active Noise Control System for Ventilation Systems, Part I: Influence of Measurement Noise on the Performance and Convergence of the Filtered-x LMS Algorithm*, International Journal of Acoustics and Vibration, **14**, 4, 188–195.
9. Leniowska L. (2006), *Effect of active vibration control of a circular plate on sound radiation*, Archives of Acoustics, **31**, 1, 77–87.
10. Leniowska L., Kos P. (2009), *Self-tuning control with regularized RLS algorithm for vibration cancellation of a circular plate*, Archives of Acoustics, **34**, 4, 613–624.
11. Lizhong X., Zhentong W. (2009), *Electromechanical Dynamics For Microplate*, International Journal of Acoustics and Vibration, **14**, 4, 12–23.

12. National Semiconductors (2000), *LM35 Precision Centigrade Temperature Sensors*, Retrived October 14t, 2010 from http://www.national.com/ds/LM/LM35.pdf.

13. Pawełczyk M. (2005), *Feedback Control of Acoustic Noise at Desired Locations*, Silesian University of Technology, Gliwice.

14. Pietrzko S.J. (2009), *Contributions to Noise and Vibration Control Technology*, AGH – University of Science and Technology Press, Kraków.

15. Smart Material (2010), *MFC*, Retrieved October 14th, 2010 from http://www.smart-material.com/Smart-choice.php?from=MFC.

16. Tanaka N. (2009), *Cluster Control of Distributed-Parameter Structures*, International Journal of Acoustics and Vibration, **14**, 1, 24–34.

17. Tawfik M., Baz A. (2004), *Experimental and Spectral Finite Element Study of Plates with Shunted Piezoelectric Patches*, International Journal of Acoustics and Vibration, **9**, 2, 87–97.

18. Wiciak J. (2008), *Sound radiation by set of L-jointed plates with four pairs of piezoelectric elements*, The European Physical Journal Special Topics, **154**, 1, 229–233.